Ultra-fast B_1^+ Mapping allows Speeding up RF Shimming in Body MRI at 3T

Alois Martin Sprinkart[1,2], Georg Schmitz[2], Frank Träber[1], Wolfgang Block[1], Jürgen Gieseke[3], Hans Schild[1], Peter Börnert[4,5], and Kay Nehrke[4]
[1]*Dept. of Radiology, University of Bonn, Bonn, Germany,* [2]*Institute of Medical Engineering, Ruhr-University Bochum, Bochum, Germany,* [3]*Philips Healthcare, Hamburg, Germany,* [4]*Philips Research Laboratory, Hamburg, Germany,* [5]*Dept. of Radiology, LUMC, Leiden, Netherlands*

Introduction

The application of radiofrequency (RF)- shimming in clinical routine has led to a significant improvement in image quality and diagnostic confidence in body MRI at 3T[1-4]. To facilitate patient adaptive RF-shimming, a separate $\mathbf{B_1^+}$ map has to be acquired for each of the employed RF transmit (TX) channels prior to the acquisition of the diagnostic imaging sequences. Based on the information about the individual transmit coil sensitivities, channel-dependent complex weighting factors are determined to homogenize the $\mathbf{B_1^+}$ field. This $\mathbf{B_1^+}$ calibration procedure requires up to two long breath-hold acquisitions when either double-angle (DA)[5] or actual-flip-angle-imaging (AFI)[6] methods are applied, which are currently commonly used for this purpose[1-4]. The recently proposed $\mathbf{B_1^+}$ mapping approach DREAM[7], however, allows $\mathbf{B_1^+}$ mapping in a single shot, and therefore, has the potential to significantly speed up RF shimming in clinical routine. However, up to now a verification of the practical applicability of DREAM for $\mathbf{B_1^+}$ calibration in a clinical setting is lacking. Therefore, the aim of our study was to compare the flip angle accuracy and $\mathbf{B_1^+}$ homogeneity achieved by RF-shimming based on calibration data acquired with DREAM, DA and AFI.

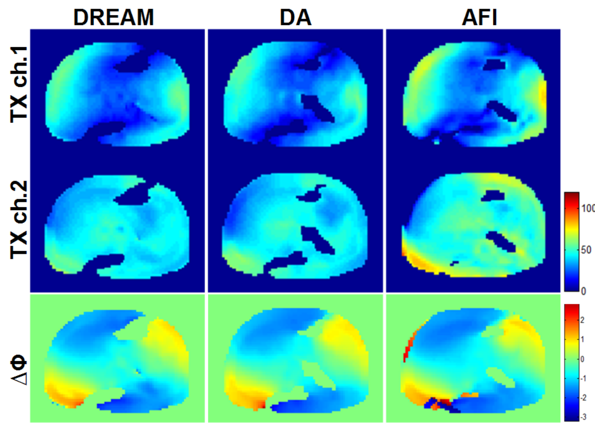

Fig. 1. **$\mathbf{B_1^+}$ calibration data** obtained with DREAM, DA and AFI in a 26y old volunteer. The $\mathbf{B_1^+}$ magnitude of the two TX channels is shown in the upper two rows and given in % of the nominal flip angle. Row 3 shows the relative phase between the two channels in radians. Based on these complex valued information on the RF transmit fields, optimal channel-dependent complex weighting factors are determined, which homogenizes the active $\mathbf{B_1^+}$ field. While DREAM and DA yield almost identical $\mathbf{B_1^+}$ calibration data, AFI yields slightly higher values for the flip angle. Note that the maps were automatically masked by the scanner software for use in the optimization algorithm.

Methods

Ten healthy volunteers with written informed consent were included in this prospective study, which was approved by the institutional review board. The study was conducted on a clinical dual-transmit 3T MRI system (Ingenia, Philips Healthcare, Best, The Netherlands). Three $\mathbf{B_1^+}$ calibration scans (FOV= 464x530mm^2 , slice thickness= 20mm, acq./rec. matrix= 64x64 / 112x112, scan percentage: 82%) centred in the upper abdomen were acquired in a single breath-hold (DREAM and DA) and two breath-holds (AFI), respectively. Specific sequence parameters were as follows: DREAM: TR= 3.7ms, TE_{FID}/TE_{STE}= 2.3ms/ 1.2ms, T_S= 3.5 ms, STEAM flip angle α= 60°, imaging flip angle β= 10°, number of scans averaged (NSA)= 1, DA: TR= 755ms, TE= 40ms, α=130°, saturation delay= 650ms, NSA = 2, AFI: TR_1/TR_2= 20ms/100ms, TE= 2.2ms , NSA = 1. Total acquisition time was 1 s for DREAM, 15 s for DA and 31 s for AFI.

The target volume for RF shim optimization was restricted to the torso. The standard RF shim algorithm of the scanner software was used to compute optimal channel-dependent complex weights that minimize the coefficient of variation (cv = std/mean) in $|\mathbf{B_1^+}|$, taking regulatory SAR constraints into account.

The active $\mathbf{B_1^+}$ field before and after RF-shimming was monitored with AFI using the same sequence parameters as for the calibration scans. For evaluation of the shim results, mean $|\mathbf{B_1^+}|$ (expressed in percentage of the nominal flip angle) and the coefficient of variation in $|\mathbf{B_1^+}|$ were determined to serve as measures for flip angle accuracy and $\mathbf{B_1^+}$ homogeneity, respectively.

Results

Good quality $\mathbf{B_1^+}$ calibration data have been obtained with each of the three investigated $\mathbf{B_1^+}$ mapping methods in all volunteers (c.f. Fig. 1). Figure 2 shows an example of obtained shim results. By RF shimming, the coefficient of variation in $|\mathbf{B_1^+}|$ was reduced from 26.6±1.8% (mean±std of all subjects studied) to 16.4±2.1% with DREAM-based calibration, to 16.5±1.8% with DA-based calibration and to 17.2±1.5% with AFI-based calibration. Mean flip angle without RF shimming was 76.1±3.3% and was improved to 102.4±8.2%, 103.1±9.6% and 94.0±5.4% with RF shimming based on DREAM, DA and AFI calibration data, respectively.

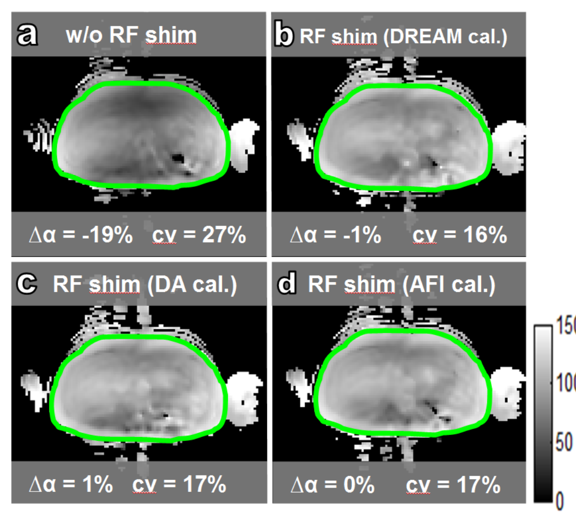

Fig. 2. **Comparison of shim results** in a 36y old volunteer: active $|\mathbf{B_1^+}|$ field without RF shimming (a), with RF shimming based on $\mathbf{B_1^+}$ calibration data acquired with DREAM (b), DA (c), and AFI (d). Note that good RF shimming results are achieved for all of the investigated $\mathbf{B_1^+}$ mapping methods (Δα: mean deviation from nominal flip angle, cv: coefficient of variation in $|\mathbf{B_1^+}|$). $\mathbf{B_1^+}$ maps were acquired with AFI. The green border marks the region (torso) for evaluation of the flip angle accuracy and the $\mathbf{B_1^+}$ homogeneity.

Discussion

$\mathbf{B_1^+}$ calibration based on DREAM yields good quality RF shim results similar to those currently achieved with DA- and AFI- based $\mathbf{B_1^+}$ calibration. Since DREAM allows single-shot $\mathbf{B_1^+}$ mapping, time requirements for RF shimming on a dual source system reduces to only one second, when DREAM is used for calibration. While this study was performed in volunteers only, in a future work it will have to be evaluated, whether these results are also valid in patients, where e.g. ascites hampers RF penetration.

References

1. Willinek WA et al., Radiology 2010;256:966-975. **2**. Kukuk GM et al., Radiology 2011;259:421-428. **3**. Nelles M et al., Radiology 2010;257, 743-753. **4**. Pazahr S et al., Radiology 2012;265, 591-599. **5**. Cunningham, CH et al. MRM 2006;55:1326-1333. **6**. Yarnykh VL, MRM 2007;57:192-200. **7**. Nehrke K et al. MRM 2012;68:1517-1526.